International Journal of Applied, Physical and Bio-Chemistry Research (IJAPBCR)
Vol.2, Issue 1 Mar(2012) 1-32

ADSORPTION OF ENANTIOMERS ON METAL SURFACES: APPLICATION TO D- AND L-ALANINE ON CU, NI AND ZN ELECTRODES

S. Harinipriya [a*], V. Sudha [b], M. V. Sangaranarayanan* [b] and E. J. Padma Malar[c]

[a]*Center for energy, Indian Institute of Technology Rajasthan, Jodhpur, 342011, India*

[b]*Department of Chemistry, Indian Institute of Technology – Madras, 6000 36, India*

[c]*Department of Physical Chemistry, University of Madras 6000 25, India*

* corresponding author: shpriya@iitj.ac.in

ABSTRACT

Different techniques have been developed for enantiomeric separation in order to meet the need for optically pure materials in the pharmaceutical, fine chemical and electronic industries. The present study explores the extent of selective adsorption of chiral compounds on metal electrodes, from knowledge of adsorption energy difference between D- and L- enantiomers. An entirely new simulation strategy is employed via Monte-Carlo method to evaluate the adsorption energy difference between D- and L- enantiomers. This methodology also yields the amount of each species adsorbed for a chosen electrode potential. The adsorption of tetrameric D- and L- alanines at Cu, Ni and Zn electrodes as well as in solution are studied using their stabilization energies obtained at the B3LYP/6-31G optimized structures. Subsequently these stabilization energies are employed as input parameters to estimate the adsorption energy difference between D- and L-alanine tetramers. The adsorption energy difference obtained from the simulation is found to be identical with the umbrella inversion energy for the lone pair of electrons on the amino group. It is demonstrated that, in a racemic mixture, only the D–alanine tetramer gets adsorbed predominantly on

Cu, Ni and Zn while the adsorption of the L–species is more facile than the D-form when the corresponding pure enantiomer is employed. The origin of the preferential adsorption of D-enantiomer from a racemic mixture is interpreted using the computation of the molar volumes of the optimized geometries. Thus the evaluation of the adsorption energy of chiral compounds on metal electrodes can lead to valuable predictions for separation of optically active pure enantiomers.

INTRODUCTION

Perpetual growth in annual demand for enantiomerically pure chiral compounds occurs in the chemical, biochemical and pharmaceutical industries[1], the main focus being the study of (i) enantiospecific heterogeneous catalysis, bio-functionality, bio-toxicity effects in biochemical phenomena and (ii) pharmaceuticals development and manufacturing, associated with different enantiomers in *vivo*. Initial interest in enantiospecific heterogeneous catalysis is traced to the study of Orito reaction [2], carried out nearly two decades ago, wherein cinchonidine was employed as a chiral modifier for platinum surfaces in ± ketoester hydrogenation reactions. Subsequently the above reaction is applied to different reactants and modifiers[3]. An alternate approach in the development of technology for enantiospecific production of useful compounds is based on the chemistry of the metal catalyst itself, rather than the reactants and modifiers chosen. The examination and initial nomenclature suggestions for chiral surface sites on metal surfaces such as the chiral kinks associated with the Pt(643) surface may offer the key to enantiomeric selection in adsorbates. It was the pioneering work of Sholl[4] employing various crystal faces of Pt such as Pt(111) and Pt(643), on the behaviour of dimethylcyclopropane and limonene, through umbrella-sampled Monte Carlo (MC) simulation techniques that pointed out the feasibility of enantiomeric selection in adsorption and desorption studies. The results are in agreement with the analysis of Gellman et al [5]. which indicated that there should be appreciable experimentally detectable differences

in the enantiospecificity of the surface in the Temperature Programmed Desorption (TPD), at least for some compounds. Attard et al[6] provided complementary results pertaining to the theory of enantiospecificity on naturally chiral metal surfaces. The analysis of glucose adsorbed on a variety of Pt single crystal faces as working electrodes for voltammetric study led to large, clearly discernable results in the differing permutations of glucose enantiomers and surface chirality for a given crystal face. These results yielded a different nomenclature system for the chiral surfaces, a refinement on the projections made by Gellman et al. This work along with the corresponding nomenclature protocol is still dominant in the area of chiral metal surface chemistry.

Hovarth and Gellman [7] observed that propylene oxide and methylcyclohexane underwent adsorption – desorption phenomena on chiral copper surfaces Cu(111) and Cu(643). Once again, for certain permutations of binding of species such as R–3–methylcyclohexane on Cu(643) surface, there are observable enantiospecific effects associated with the kink site. As mentioned earlier, another scenario of interest involves chiral molecules adsorbed on achiral surfaces such as the (100), (110), or (111) face of an fcc crystal, for example glycine on Cu(001) surfaces [8]. It is also possible to induce chirality effects in pro-chiral molecules such as glycine adsorbed on achiral lattice faces. It was observed that the rate of deposition of adsorbate is a critical driving force in dictating the magnitude and nature of surface rearrangement.

Apart from glycine, interfacial behaviour of other aminoacids such as alanine, aspargine, aspartic acid etc have also been studied. Zhao et al [8**]** have investigated the adsorption behavior of amino acids on the Cu(100) (or Cu(001 according to [8]). Amino acids with large alkyl groups characterized by carboxyl (L-aspargine) or carbonyl-amine (L-aspartic acid) do not organize into assembled patterns and domains on the surface. In contrast, other amino acids such as tryptophan exhibit organized assembly during adsorption. A typical analysis by Zhao et al demonstrated the self-assembly of L-tryptophan on Cu

(100) using Scanning Tunneling Microscopy (STM). The carboxyl group of the L-tryptophanate ions as well as the indole group bond to the Cu (100) surface with different monolayer coverage. The driving force for this behavior is attributed to hydrogen bonding between the ions, as well as π- stacking in parallel indole groups.

A systematic study of adsorption of amino acids on different single crystals is especially crucial since (i) most organic molecules hitherto studied are either planar or rigid in contrast to amino acids which are flexible and chiral, possessing several active functional groups thus enabling us to explore the influence of different intermolecular and molecule-substrate interactions on self-assembly; (ii) proteins consisting of amino acids constitute nearly 50% of the dry mass of cells and hence understanding the adsorption mechanism of amino acids on inorganic surfaces is necessary for the development of biocompatible materials and (iii) proteins can impose order on mineral phases so as to produce the remarkable properties of bones, teeth and shells. For developing new materials, it is therefore imperative to commence the investigation of adsorption of amino acids on inorganic single crystal surfaces from an entirely new perspective. The advance of computing power and technology in recent years has allowed the application of Density Functional Theory (DFT) to larger systems, in more realistic timescales. This advance has prompted the collaboration of experimental and theoretical work at simultaneous or nearly simultaneous time frames. It is now well known that DFT in conjunction with experimental studies can play a valuable role in comprehending the adsorption behaviour of enantiomers on various substrates.

In the present work, the stabilization energies of the tetrameric structures of D- and L- alanine at Cu, Ni and Zn electrodes as well as at the solution are studied with the help of molecular dynamics simulation using DFT calculations at B3LYP/6-31G level. A new simulation strategy is proposed for estimating the adsorption energy difference between D- and L-configurations using the

stabilization energies as the input parameters. The present simulation technique also yields the amount of each species adsorbed for a chosen electrode potential.

SALIENT FEATURES OF THE METHODOLOGY

Molecular Dynamics (MD) and Monte Carlo (MC) simulations

The MD simulation study for binding energies makes use of Hartree – Fock – Density Functional Theory (DFT) results obtained with Becke's three-parameter hybrid-exchange functional and the gradient-corrected non-local correlation functional of Lee, Yang and Parr (B3LYP)[9], using the Gaussian 03 software[10]. All electron calculations using the split valence basis set were performed at B3LYP/6-31G level. The floppy molecules under study exist in shallow potentials and extensive computer time is needed for structural optimization due to very slow convergence. We imposed stringent convergence criteria using SCF = TIGHT option, in order to achieve Self-Consistent- Field (SCF) convergence[11]. Because of the large amount of computer time required to arrive at the optimized geometries, the basis set for structural optimization was restricted at the split valence level 6-31G, although 6-31G* basis set which includes polarization correction is known to be more accurate[11]. However, single point B3LYP/6-31G*//B3LYP/6-31G calculations were done at the B3LYP/6-31G optimized geometries.

The alanine molecules at the center of the cubic box were assumed to jump to a distance of 0.5 Å, on account of the applied potential (ϕ_{app}), along with its hydrogen bonded pairs and move progressively to the surface of the cube (representing the metal surface) and adsorb on the surface of the metal. The simulation is employed for obtaining (i) the number of molecules that arrive at the surface of the cube (metal) and (ii) the energy required for adsorption of each configuration employing the energy ratio as the criterion while generating

random numbers for the analysis. From these values we arrive at the adsorption energy difference between the D- and L- species as shown below.

The *essential* input parameters required for the present analysis are (i) the stabilization energies of the tetrameric D- and L- alanine in the bulk and at the metal electrode obtained by the DFT calculations and (ii) the conformation energy of the corresponding species on the metal surface. Using these two parameters, an explicit expression for the total energy required for the molecules to get adsorbed on the metal surface and their electrochemical potential at the metal surface are formulated. Before the simulation, the molecules are allowed to equilibrate for 0.03 pico sec, by rigidly allowing the molecules to move a particular distance (Δd) in the time ratio t_{exp}/t_{eq}, see eqn (5).

SIMULATION DETAILS

(A) Molecular Dynamics Simulation

Since the lowest energy conformations are the main focus of the study, we generated the D- and L-alanine tetramer conformations with the maximum number of intermolecular H-bonds. Starting from the optimized monomer conformation (both L- and D-), the second, third and fourth alanine units were oriented such that maximum number of H-bonds exist between the alanines. These conformations were then subjected to complete structural optimization at B3LYP/6-31G level. The suitability of the DFT method to yield reliable predictions on H-bonding interactions is established in earlier studies[12-18]. Since the starting structures are chosen with maximum H-bonding interactions, the resulting optimized conformations are near the global minima. With the intermolecular H-bonding fixed, the conformational freedom in adopting different possible orientations with reference to the constituent alanine units is curtailed. At the optimized $(\text{D-ala})_4$ and $(\text{L-ala})_4$ geometries, the two metal atoms (M = Cu, Ni and Zn, as the case may be) were added and once again subjected to complete structural optimization. At the optimized geometries, we performed

natural bond orbital (NBO) analysis[19-21] and the covalent interactions were examined using covalent bond orders[22]. Vibrational frequencies were calculated at the B3LYP/6-31G optimized geometries to ascertain their true minima status. No imaginary vibrational frequencies were present and thus the optimized structures were confirmed to be true minima in the potential energy surface. Zero-point vibrational energies (ZPE) were scaled by a factor of 0.9614 which was found suitable for B3LYP/6-31G* calculations[23]. Single point energy calculations were carried out at the B3LYP/6-31G*//B3LYP/6-31G level by making use of the B3LYP/6-31G optimized geometries. The total energies and the zero-point vibrational energies are presented in Table S1 in the Supporting Information. Stabilization energy of a given system ΔE is obtained by subtracting the total energies of the components from the total energy of the system as shown below:

$$\Delta E\ [(\text{D-ala})_4]=E[(\text{D-ala})_4]-4xE(\text{D-ala}) \quad (1)$$

$$\Delta E\ [(\text{L-ala})_4]=E[(\text{L-ala})_4]-4xE(\text{L-ala}) \quad (2)$$

$$\Delta E\ [(\text{D-ala})_4M_2]=E[(\text{D-ala})_4M_2]-4xE(\text{D-ala})-E(M_2) \quad (3)$$

$$\Delta E\ [(\text{L-ala})_4M_2]=E[(\text{L-ala})_4M_2]-4xE(\text{L-ala})-E(M_2) \quad (4)$$

(B) Monte Carlo simulation

The simulation was carried out in the NTP ensemble and the system consisting of the alanine molecules was placed in a cubic box of length l Å. The simulation is performed for the chosen number density (molecules/cm^3) of alanine. Boundary conditions were employed and the cube was confined (rigidly fixed) along z–axis. The molecules were initially placed at the center of the cube where it was equilibrated for 0.03 pico seconds whereas the experimental time for the molecules to feel the applied potential is 1 sec (vide infra) and allowed to move in x and y direction depending upon the initial displacement of

the molecule. The distance (d_{total}) traveled by the molecules will be half the length of the cube ($d_{total} = l/2$).

Choice of input parameters for the Monte Carlo Simulation

(i) The mean displacement of each alanine molecule in every 0.03 pico secs is Δd . Initially, before applying external potential ϕ_{app} , Δd is assumed to be zero (the molecules are at the center of the cube). For every value of the applied potential (ϕ_{app}), Δd is calculated from an empirical expression

$$\Delta d = t_{\exp} * x \Big/ t_{eq} \tag{5}$$

where ' x ' denotes the expected displacement of the molecules (here assumed as half of the hydrogen bonding distance ($0.5A^0$) since in each displacement of the molecules the hydrogen bond is broken and formed simultaneously), $t_{\exp}$ being the experimental time of one sec[24] and t_{eq} is the equilibration time during simulation. The ratio t_{exp}/t_{eq} will provide the equilibration of the structures when the potential ϕ_{app} is applied. Here the expected displacement is assumed to be half the hydrogen bonding distance, since the only driving force for the tetramer structures is the hydrogen bonding between the four individual molecules. The hydrogen bonding distance is divided by two since during the simulation the alanine tetramers are allowed to move in either of the two directions x and y. While Δd is the expected displacement for each alanine tetramer from its original position, the actual displacement ' d ' will be larger than this on account of the hydrogen–bonding between the four alanine molecules.

Hence we write

$$d = d_{HB} + \Delta d \tag{6}$$

where d_{HB} is the hydrogen bonding distance (assumed to be equal to 1 A^0 in the simulation; although the hydrogen bonding distance may extend to 2 A^0, the latter value when employed leads to ~ 5% difference in computed energies).

(ii) The energy (E_{mis}) involved in the displacement of the tetramer from its original position to a new position inside the cubic box depends on (i) the total distance covered by the species for reaching the metal surface from its new position and (ii) the expected displacement on account of the applied potential.

Hence, E_{mis} can be written as

$$E_{mis} = \left(\frac{\Delta d * \phi_{app}}{d_{totalrem}} \right) \tag{7}$$

where $d_{totalrem}$ is the remaining distance the molecules have to travel from their new position to reach the metal surface (surface of the cube) subsequent to applying the potential ϕ_{app}. $d_{totalrem}$ is expressed as

$$d_{totalrem} = d_{total} - d \tag{8}$$

(iii) the total energy involved in the orientation and the displacement of the tetramer from its initial position to the new position can now be written as

$$E_{iD} = \left(\frac{E_{D-Ala} * d_{totalrem}}{d} \right) + E_{mis} \tag{9}$$

$$E_{iL} = \left(\frac{E_{L-Ala} * d_{totalrem}}{d} \right) + E_{mis} \tag{10}$$

where E_{D-Ala} and E_{L-Ala} are the stabilization energies for the tetramers of D- and L- alanine in bulk, respectively, for the chosen metal surface.

(iv) The electrochemical potentials involved in the adsorption process are represented as

$$\mu_D = E_{iD} - \phi_{app} \tag{11}$$

$$\mu_L = E_{iL} - \phi_{app} \tag{12}$$

where μ_D and μ_L refer to the electrochemical potential for D- and L-species respectively.

Simulation methodology

In order to obtain the number of alanine molecules that reach the surface of the cube (equivalently the metal surface) random numbers are generated employing energy criterion as follows:

$$ir(j) > \exp(-(E_{iL} / E_{iD})) \tag{13}$$

Eqn (13) yields the number of D- or L-alanine molecules reaching the metal surface. From the number of alanine molecules that reach the metal surface, the total energy required for their displacement from the center of the cube to the surface follows as

$$E_{iconfD} = (N_{sur} / N_{D-Ala}) * E_{iD} \tag{14}$$

and

$$E_{iconfL} = (N_{sur} / N_{L-Ala}) * E_{iL} \tag{15}$$

where N_{sur} denotes the number of molecules reaching the surface while $N_{D\text{-}Ala}$ and $N_{L\text{-}Ala}$ refer to the number of D- and L-alanine molecules after each displacement. E_{iconfD} and E_{iconfL} indicate respectively the adsorption energies of D- and L- alanine on the metal surface. However, for obtaining the number of D- or L- alanine molecules starting from a racemic mixture, the following energy criterion is employed:

$$ir(j1) >= \exp\left(\frac{-(E_{D-ala} + E_{totalD})}{E_{totalD}}\right) \tag{16}$$

$$ir(j2) >= \exp\left(\frac{-(E_{L-ala} + E_{totalL})}{E_{totalL}}\right) \tag{17}$$

If the generated random number satisfies eqn 16, then D-alanine adsorbs on the metal surface, E_{totalD} being the adsorption energy of the D-alanine molecules obtained from eqns (13) and (14). On the other hand, if the generated random number satisfies eqn 17, then L-Alanine gets adsorbed, E_{totalL} being the adsorption energy of L-alanine on the metal. Scheme1 indicates the steps involved in the simulation methodology.

RESULTS AND DISCUSSION

(A) Molecular dynamics simulation

(i) Hydrogen bonding interactions in the tetrameric clusters of D-alanine and L – alanine

The fully optimized geometries of the tetrameric alanines shown in Figure 1 reveal the formation of three intermolecular H-bonds between the electropositive amino hydrogen of one of the D-alanines with the acceptor oxygen atom of neighboring D-alanine within the units D-ala$_1$, D-ala$_2$ and D-

ala_3. Further, these structures indicate the existence of a strong interaction between the nitrogen of D-ala_3 and the carboxylic hydrogen of D-ala_4. Eventually the hydrogen atom H_4 is pulled towards the nitrogen of D-ala_3, N_3, leading to covalent bond formation with bond length of 1.092 Å, which is about 0.08 Å longer than the B3LYP/6-31G predicted N-H bond length in alanine. Similarly, N_4 of D-ala_4 forms a covalent bond with the carboxylic hydrogen of D-ala_3. Consequently the bond lengths between O_3 and H_3 as well as O_4 and H_4 are elongated to 1.568 and 1.534 Å respectively and are characteristic of H-bond formation. Thus there are 5 intermolecular H-bonds in the cluster of $(D\text{-ala})_4$. The lengths of these H-bonds lie in the range 1.53 – 2.12 Å and are shown in Figure 1 as broken lines. The bond angles D-H…A for these intermolecular H-bonding interactions are found to be 155-169° (Table 1). The directionality and the lengths of these H-bonds indicate moderately strong H-bonds. The formation of covalent bonds N_3-H_4 and N_4-H_3 causes considerable structural reorganization in the residues D-ala_3 and D-ala_4. This reorganization leads to the formation of intramolecular H-bonds $N_3H'\ldots O_3$ in D-ala_3 and $N_4H'\ldots O_4$ in D-ala_4 with lengths of 2.02 and 1.93 Å respectively. These two H-bonds have bent-structures with bond angles of 109.5° and 113.9°, indicating that they are weak bonds. The stabilization energies listed in Table 3 shows that the hydrogen bonding interactions in the tetrameric D-alanine cluster increases the stability of the system by 34.0 kcal/mol relative to the four non-interacting D- alanine monomers, according to B3LYP/6-31G level calculations with ZPE correction. The stabilization energy is predicted to be -39.6 kcal/mol when ZPE correction is not taken into account. The results are consistent with the presence of 7 H-bonds in the cluster indicating that the average H-bond energy is 4.9 - 5.7 kcal/mol. However, B3LYP/6-31G*// B3LYP/6-31G predict a smaller stabilization energy of -21.7 kcal/mol. The calculations suggest that in the tetramer of L-alanine, the geometry of the individual alanine molecules are not

altered significantly. From Figure 1, it is inferred that three intermolecular H-bonds contribute predominantly to the stability of the L-tetramer.

Scheme 1: Estimation of the adsorption energy difference between D and L alanine molecules

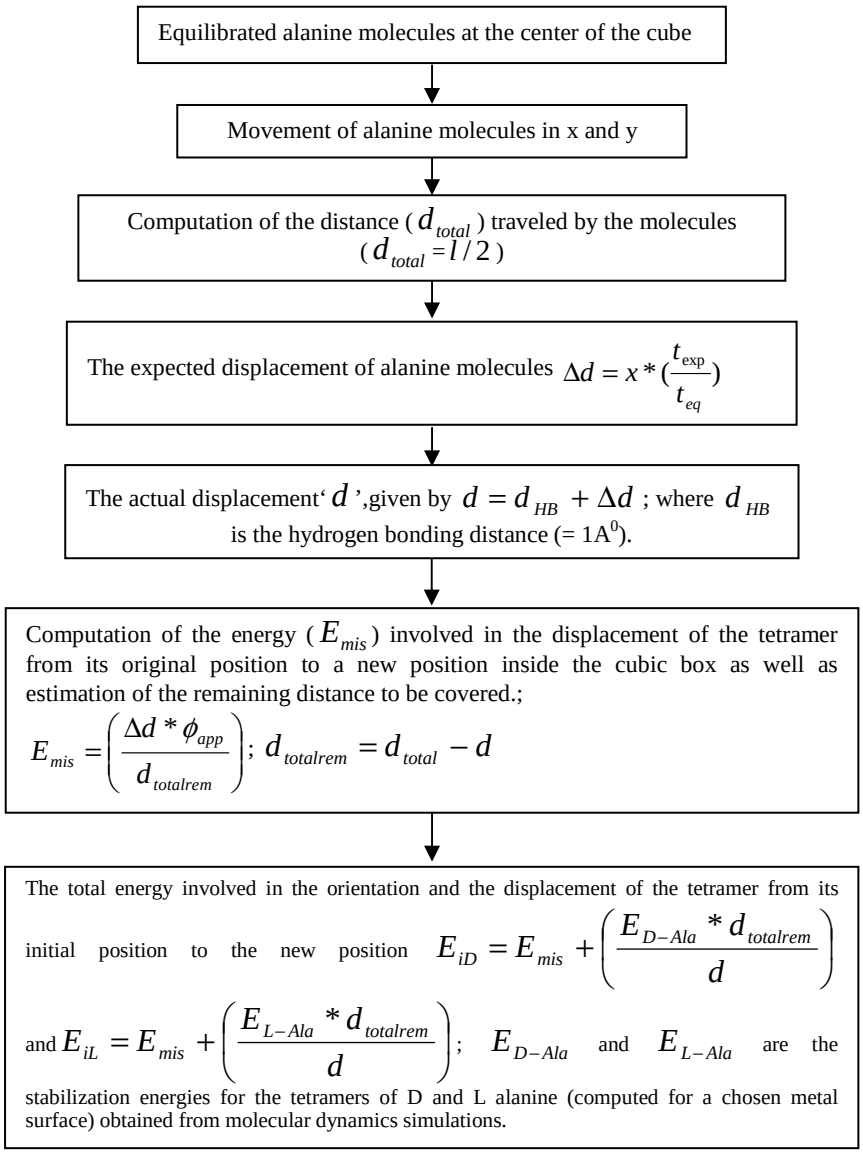

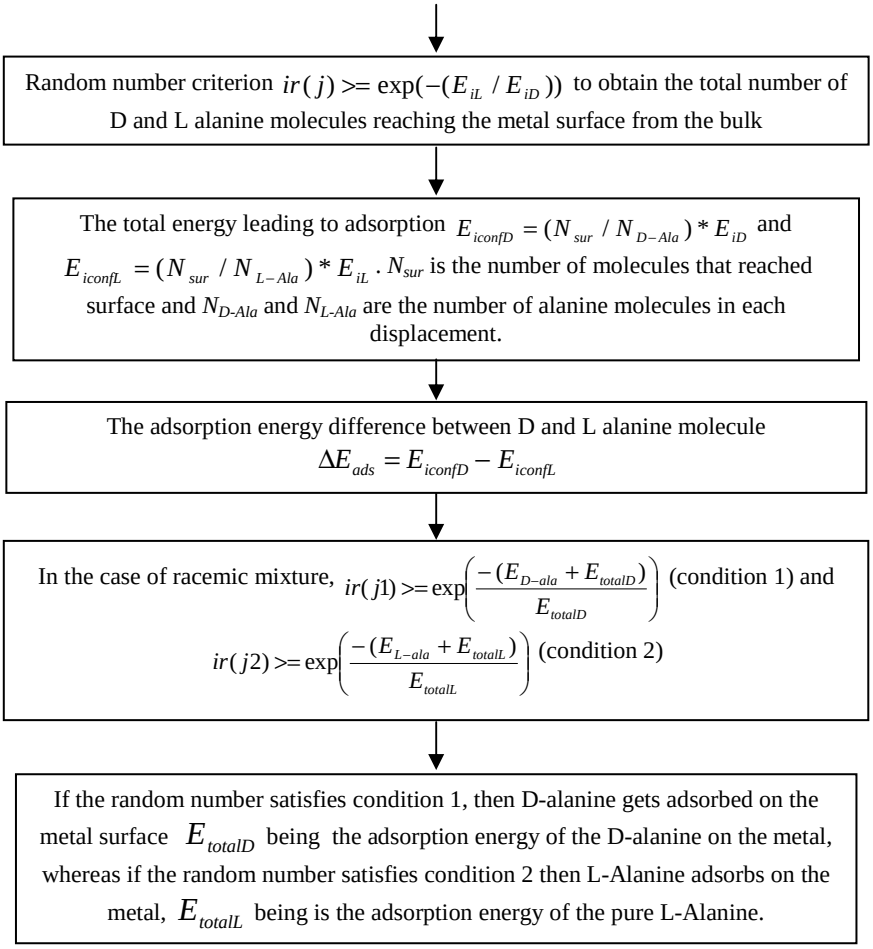
Random number criterion $ir(j) >= \exp(-(E_{iL} / E_{iD}))$ to obtain the total number of D and L alanine molecules reaching the metal surface from the bulk
The total energy leading to adsorption $E_{iconfD} = (N_{sur} / N_{D-Ala}) * E_{iD}$ and $E_{iconfL} = (N_{sur} / N_{L-Ala}) * E_{iL}$. N_{sur} is the number of molecules that reached surface and $N_{D\text{-}Ala}$ and $N_{L\text{-}Ala}$ are the number of alanine molecules in each displacement.
The adsorption energy difference between D and L alanine molecule $\Delta E_{ads} = E_{iconfD} - E_{iconfL}$
In the case of racemic mixture, $ir(j1) >= \exp\left(\frac{-(E_{D-ala} + E_{totalD})}{E_{totalD}}\right)$ (condition 1) and $ir(j2) >= \exp\left(\frac{-(E_{L-ala} + E_{totalL})}{E_{totalL}}\right)$ (condition 2)
If the random number satisfies condition 1, then D-alanine gets adsorbed on the metal surface E_{totalD} being the adsorption energy of the D-alanine on the metal, whereas if the random number satisfies condition 2 then L-Alanine adsorbs on the metal, E_{totalL} being is the adsorption energy of the pure L-Alanine.

Table 1 : Directionality of the hydrogen bond formation in the B3LYP/6-31G optimized geometries of D-alanine tetramer and its bimetallic complexes: The hydrogen bond angles D-H…A are given in degrees

H-bond angle	$(D\text{-}ala)_4$	$(D\text{-}ala)_4Ni_2$	$(D\text{-}ala)_4Cu_2$	$(D\text{-}ala)_4Zn_2$
N_1-H…O_2	168.6	169.4	170.1	170.3
N_2-H…O_1'	154.5	151.9	151.7	154.4
N_2-H'…O_3'	161.2	160.8	161.5	164.2
O_3…H_3-N_4	156.0	157.2	161.7	162.8
O_4…H_4-N_3	158.7	165.6	162.1	115.0
N_3-H'…O_3	109.5	105.9	110.0	116.0
N_4-H'…O_4	113.9	115.8	112.8	109.3

The lengths and angles of these H-bonds are about 2.15 Å and 150° (Table 2). It is seen from Table 3, that the energy of the tetramer is lowered by 8 kcal/mol as compared to the energy of 4 non-interacting alanines, indicating that the stability per H-bond is about 2.7 kcal/mol, according to B3LYP/6-31G calculations with ZPE correction. The cluster is predicted to be marginally more stable (8.4 kal/mol) at B3LYP/6-31G*// B3LYP/6-31G level.

Table 2 : Directionality of hydrogen bond formation in the B3LYP/6-31G optimized geometries of tetramer of L-alanine and its bimetallic complexes: The hydrogen bond angles D-H…A are given in degrees.

H-bond angles	$(L\text{-ala})_4$	$(L\text{-ala})_4Ni_2$	$(L\text{-ala})_4Cu_2$	$(L\text{-ala})_4Zn_2$
N_1-H…O_2'	150.2	149.2	149.5	147.3
N_2-H…O_3'	149.1	135.9	134.4	153.5
N_3-H…O_4'	150.5	146.9	139.2	
N_3-H…O_4				169.7
N_3-H'…O_2				143.8

Table 3 : Stabilization energies (kcal/mol) of D-alanine and L-alanine in the bulk as well as on the bimetallic complexes of Ni, Cu and Zn

	B3LYP/6-31G corrected for ZPE	B3LYP/6-31G	B3LYP/6-31G*// B3LYP/6-31G
$(D\text{-ala})_4$	-34.0	-39.6	-21.7
$(L\text{-ala})_4$	-8.0	-10.0	-8.4
$(D\text{-ala})_4Ni_2$	-120.3	-125.3	-105.8
$(L\text{-ala})_4Ni_{2-}$	-157.8	-157.8	-154.7
$(D\text{-ala})_4Cu_2$	-80.5	-85.8	-68.9
$(L\text{-ala})_4Cu_2$	-136.9	-138.2	-132. 3
$(D\text{-ala})_4Zn_2$	-56.8	-62.5	-46.3
$(L\text{-ala})_4Zn_2$	-72.5	-73.6	-65.5

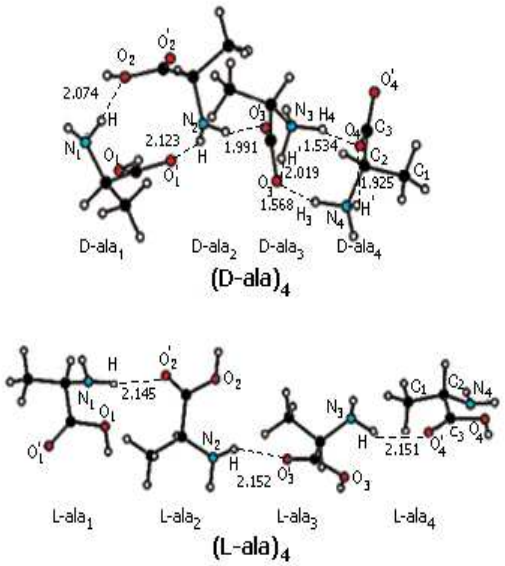

Figure 1 : B3LYP/6-31G optimized geometries of $(D\text{-ala})_4$ and $(L\text{-ala})_4$. Labeling of atoms and the alanine units followed in the present study are also depicted.

Analysis of the optimized geometries of bimetallic complexes of $(D\text{-ala})_4$ cluster (Figure 2) indicates that the metal centers are oriented closer to the carboxylic group of the $D\text{-ala}_4$ unit. Thus the alanine units 1, 2 and 3 do not undergo any significant structural change from that of the tetrameric cluster $(D\text{-ala})_4$. All the H-bonding interactions present in $(D\text{-ala})_4$ are retained in the complexes $(D\text{-ala})_4M_2$ with maximum deviation of about 0.04 Å in the H-bond lengths and 5° in the H-bond angles (Table 1), in general. Somewhat larger deviations in the H-bonding parameters are observed when $D\text{-ala}_4$ is involved, due to the proximity of the metal centers. The metal atoms exhibit significant covalent interactions with the oxygen and carbon centers of the carboxylic group

of D-ala$_4$ since they are located closer to them, particularly in the Ni and Cu complexes. The significant structural parameters indicating the interactions around the metal centers are listed in Table 4. The covalent bond orders are shown inside parenthesis.

Table 4 : Selected structural parameters in the B3LYP/6-31G optimized geometries of tetramer of D-alanine and its bimetallic complexes: bond lengths in Å, bond angles and dihedral angles in degrees. Covalent bond orders are given inside parenthesis

Parameter	(D-ala)$_4$	(D-ala)$_4$Ni$_2$	(D-ala)$_4$Cu$_2$	(D-ala)$_4$Zn$_2$
M_1-M_2		2.143 (1.055)	2.151 (0.941)	2.592 (0.185)
M_1…O_4		2.647 (0.156)	2.008 (0.123)	2.221 (.056)
M_2…O_4'		1.738 (0.635)	1.997 (0.169)	2.176 (0.062)
M_2…C_3		2.387 (0.113)	2.011 (0.398)	2.904
M_1…C_3		1.816 (0.745)	2.053 (0.365)	2.958
M_1…C_1		2.456 (0.073)	3.484	5.015
M_1…H_C		1.851 (0.093)	2.728	4.687
O_4…H_4	1.534 (0.163)	1.502 (0.189)	1.647 (0.123)	4.003
N_3-H_4	1.092 (0.579)	1.113 (0.549)	1.074 (0.614)	1.095 (.554)
N_4-H_3	1.083 (0.594)	1.099 (0.559)	1.102 (0.557)	1.100 (.564)
O_3…H_3	1.568 (0.149)	1.488 (0.177)	1.480 (0.181)	1.515 (0.177)
$C_1C_2C_3$	112.2	107.1	114.7	112.2
$C_1M_1M_2$		131.1	80.5	83.4
$M_1M_2O_4$'		82.5	92.6	79.6
$C_1C_2C_3M_2$		87.0	61.9	144.9

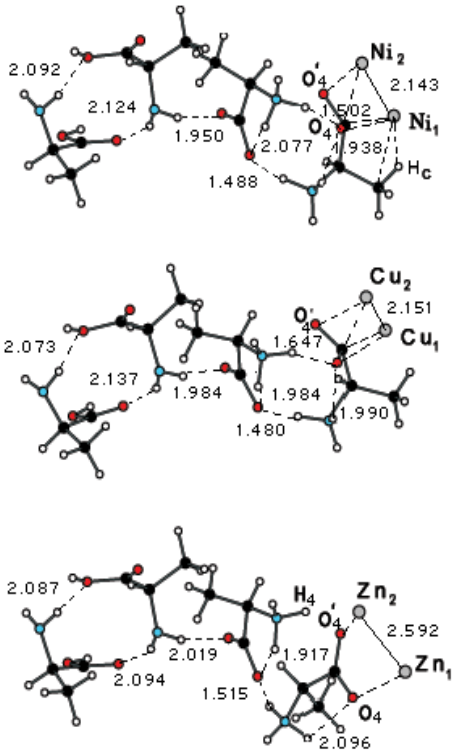

Figure 2 : B3LYP/6-31G optimized geometries of $(D\text{-ala})_4M_2$ where M refers to Ni, Cu or Zn

The calculations predict that a strong covalent interaction exists between Ni_2 and O_2' leading to bond formation with Ni_2-O_2' bond length of 1.738 Å, which is typical of Ni-O single bond. Similarly a single bond is formed between Ni_1 and C_3 having the bond length of 1.816 Å and a bond order of 0.745.

It is clear from Table 4 that the interactions between the metal atoms with $D\text{-ala}_4$ decrease in the order Ni > Cu > Zn. In the Ni complex, in addition to the interactions of Ni atoms with the carboxylic group, Ni_1 interacts with the methyl group of $D\text{-ala}_4$ which is reflected by the shorter distances, viz. $Ni_1 \ldots C_1$ = 2.456 Å and $Ni_1 \ldots H_c$ = 1.851 Å. These interactions are absent in the Cu and Zn

complexes since there exists a large separation between the metals and the methyl group.

The metal – metal bond lengths are predicted to be 2.143, 2.151 and 2.592 Å respectively for the Ni-Ni, Cu-Cu and Zn-Zn bonds in the complexes. Although the calculated bond orders show that the M_1-M_2 (M = Ni, Cu) bonds are single bonds, the Zn-Zn bonding is considerably weak with a long bond length of 2.592 Å and a small bond order (0.185). This may be due to the closed shell d^{10} configuration of Zn. Table 5 shows that the interactions of the Zn atoms with D-ala_4 is considerably lower than those of the Ni and Cu in the bimetallic complexes, as reflected by the larger distances of separation.

Table 5 : Selected structural parameters in the B3LYP/6-31G optimized geometries of tetramer of L-alanine and its bimetallic complexes: bond lengths in Å, bond angles and dihedral angles in degrees. Covalent bond orders are given inside parenthesis

Parameter	$(L\text{-}ala)_4$	$(L\text{-}ala)_4Ni_2$	$(L\text{-}ala)_4Cu_2$	$(L\text{-}ala)_4Zn_2$
M_1-M_2		2.108 (0.874)	2.225 (0.413)	2.383 (0.507)
$M_1…N_4$		2.244 (0.123)	1.926 (0.233)	2.129 (0.074)
$M_1…O_4$		1.904 (0.408)	3.111	4.237
$M_1…O_4'$		2.780	2.968	2.175
$M_2…O_4'$		1.889 (0.349)	1.943 (0.152)	2.119 (0.062)
$M_2…O_3$		1.988 (0.118)	2.061 (0.094)	2.140 (0.057)
$M_2…C_3$		2.303 (0.148)	2.658 (0.063	3.360
$M_1…C_3$		1.952 (0.390)	2.588 (0.058)	3.017
$M_1…H_4$		1.679 (0.333)	1.592 (0.384)	3.730
$M_2…H_4$		1.711 (0.314)	1.605 (0.298)	1.558 (0.519)
$O_4…H_4$	0.982 (0.150)	3.363	4.049	4.858
$C_1C_2C_3$	111.4	113.8	115.0	112.4
$C_1M_1M_2$		78.2	80.8	109.6
$M_1M_2O_4'$		88.0	90.6	57.4
$C_1C_2C_3M_2$		38.8	45.9	171.5
$C_1M_1M_2O_4'$		-50.7	-47.0	17.4

On electrode surfaces, $(D\text{-ala})_4$ gets stabilized due to the interaction with the metal. According to the B3LYP/6-31G calculations, the stabilization energies in $(D\text{-ala})_4M_2$ are -120.3, -80.5 and -56.8 kcal/mol respectively for M = Ni, Cu and Zn, when ZPE correction is added (Table 3). This lowering in the magnitude of stabilization energy is as anticipated. Thus the increase in the stabilization energy subsequent to adsorption is ~ 86, 46 and 23 kcal/mol, respectively, for the complexes of Ni, Cu and Zn at the three different levels of calculation (Table 3).

(ii) Interactions in $(L\text{-ala})_4M_2$ (M=Ni, Cu, Zn)

From the B3LYP/6-31G optimized structures of these complexes depicted in Figure 3, it is clear that the orientations of the metal atoms favor interactions with the carboxylic group and the nitrogen center N_4 of the $L\text{-ala}_4$. Unlike in the corresponding D-analogs in which the metal atoms interact only with $D\text{-ala}_4$, it is seen that in the L-complexes the metal atom M_2 is also proximal for interaction with the carboxylic oxygen O_3 of the $L\text{-ala}_3$. Thus structural parameters in the residues $L\text{-ala}_3$ and $L\text{-ala}_4$ undergo considerable reorganization. The major changes that occur in the structural parameters surrounding the metal atoms are provided in Table 5.

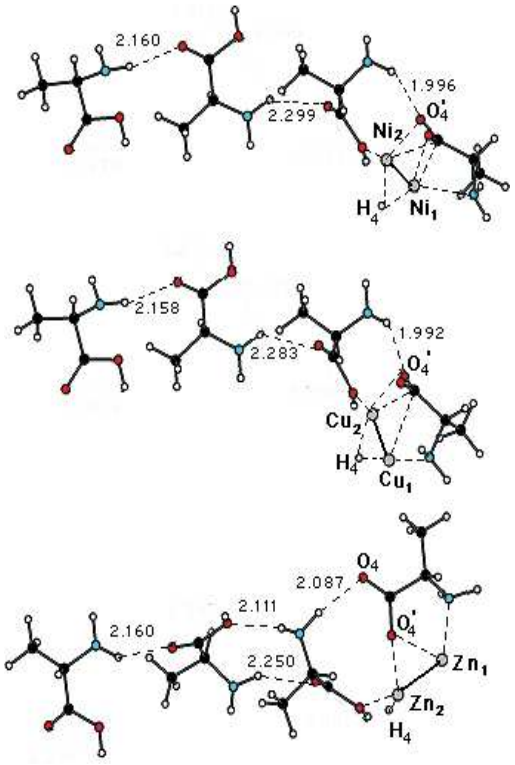

Figure 3 : B3LYP/6-31G optimized geometries of $(L\text{-ala})_4M_2$ where M refers to Ni, Cu or Zn

Figure 3 shows that the positions of the metals are favorable for bonding with oxygen atoms of the carboxylic group of $L\text{-ala}_4$. As observed in the case of $(D\text{-ala})_4M_2$ complexes, interactions between the two metal centers and the tetrameric cluster of L-alanine follows the decreasing order for Ni > Cu > Zn. This is evident from the shorter distances of 1.904, 1.889 and 1.952 Å, respectively, for $Ni_1 \ldots O_4$, $Ni_2 \ldots O_4'$ and $Ni_1 \ldots C_3$. In the case of the Cu and Zn complexes, these distances are longer and the covalent interactions are less pronounced (Table 5). Another striking observation in the $(L\text{-ala})_4M_2$ complexes is that the interactions of the metal atoms are able to push the carboxylic H_4 of $L\text{-ala}_4$ such that it is detached ($O_4\text{-}H_4$ >3.3 Å) and is located closer to the metal

atoms from the opposite side (Figure 3). The calculations reveal that in the complexes [(L-ala)$_4$M$_2$, M=Ni, Cu], the detached H_4 interacts with both M_1 and M_2 resulting in partial bond formation with bond orders in the range 0.30 – 0.38. However in the corresponding Zn complex, H_4 adopts an orientation that favors interaction with Zn_2 only. The covalent bond formation between the Zn_2 and H_4 is significant with a bond order of 0.52.

The L-ala$_4$ unit is twisted in the zinc complex and O_4' comes nearer to both the zinc atoms with a separation of 2.175 and 2.119 Å. Consequently no H-bonds exist between O_4' and the amino hydrogen of L-ala$_3$. Instead, O_4 takes part in the H-bond formation. Also, in the case of Zn complex, an additional H-bond is formed between O_2 of L-ala$_2$ with hydrogen of the amino group in L-ala$_3$. In view of the interactions between the metal atoms with L-ala$_3$ and L-ala$_4$, the H-bonds between L-ala$_2$ and L-ala$_3$ as well as that between L-ala$_3$ and L-ala$_4$ undergo changes. There is weakening of the H-bond between L-ala$_2$ and L-ala$_3$ as reflected by the increase in the H-bond length to 2.25-2.30 Å in the metal complexes as compared to the value of 2.15 Å in (L-ala)$_4$. The H-bond angle for the above bonds decreases by ~15° in the Ni and Cu complexes but the angle gets widened to 153.5° in the Zn complex (Table 2). As the interactions with the metal centers increase the negative charges on the oxygen atoms of L-ala$_4$, the H-bond between L-ala$_3$ and L-ala$_4$ is strengthened further and the H-bond length is decreased by ca. 0.15 Å. The H-bond between L-ala$_1$ and L-ala$_2$ is however, not affected in the metal complexes.

Although the L-tetramer of alanine is energetically less stable than the D-tetramer (Table 3), the present study shows that in the bimetallic complex, the two metal atoms lead to stronger stabilizing interactions with the electronegative centers in L-ala$_3$ and L-ala$_4$ units than in the D- analogue. This is evident from a comparison of distances and bond orders collected in Tables 4 and 5. Further, some of the H-bonding interactions have become stronger in the L-complex due to an increase in negative charge on oxygen center of L-ala$_4$ on account of the

influence of the metal. Thus, for example, the bonding with the two nickel centers has stabilized $(L\text{-ala})_4$ by 146 – 150 kcal/mol at different levels of computation. The corresponding stability in the case of $(D\text{-ala})_4Ni_2$ is about 84-86 kcal/mol. Thus the overall stability of the complex $(L\text{-ala})_4M_2$ has increased as compared with the corresponding $(D\text{-ala})_4M_2$ counterpart. The relative energies listed in Table 3 reveals that the increased stabilities of the bimetallic complexes of the L-tetramer over $(D\text{-ala})_4M_2$ are in the ranges 33-49, 52-63 and 11-19 kcal/mol, respectively, for M = Ni, Cu and Zn at the different levels of calculation.

B Monte Carlo Simulation studies

The Monte Carlo simulation yields the adsorption energy difference between D- and L- alanine at a chosen applied potential and identification of the predominant configuration (viz D or L) getting adsorbed in the case of a racemic mixture. Three sets of data were obtained at (i) different applied potentials (0.001V, 0.01V and 0.1V) (ii) varying sizes of the cubic box (10 Å and 15 Å) and (iii) different number densities (100 and 150). Although the number of molecules is ~ 10^2, they were chosen in order to demonstrate the adsorption energy differences even when low concentrations are employed.

We have simulated the adsorption of the pure $(D\text{-ala})_4$ as well as $(L\text{-ala})_4$ enantiomers on the metal electrodes by separately taking 100 (or 150) molecules inside a cubic box of length 10 Å (or 15 Å). Table 6 summarises the results obtained. Tables S3 to S29 of the Supporting Information provide the adsorption energy difference for each step movement of the D- and L- species from Monte Carlo simulation. It is inferred from these data that neither the applied potential nor the number of alanine molecules alters ΔE_{ads} but the nature of the metal influences its value. From Table 6, it is seen that the adsorption of the D-species is within 4 % under the different conditions while there is about a 10-fold increase in the adsorption of the L-enantiomer. The exact number of D- and L-

species getting adsorbed is dependent upon the input stabilization energies at different levels (cf. B3LYP/6-31G with and without ZPE correction or B3LYP/6-31G*//B3LYP/6-31G).

Table 6 : The number of D- and L- species that adsorb on the metal surfaces and their variation with the stabilization energies and nature of the metal surface. Applied potentials are 0.001V, 0.01V and 0.1V

M	Number of alanine tetramers and box size	Number of alanine tetramers molecules that adsorbs on the metal surface					
		B3LYP/ 6-31G with ZPE correction		B3LYP /6-31G		B3LYP/6-31G*// B3LYP/6-31G	
		D	L	D	L	D	L
Ni	100 and 10 Å	1.3	14	1.2	12.7	1.7	18.5
Cu		2.3	24.9	2.0	21.8	3.3	36.1
Zi		1.3	14	0.8	8.6	1.7	18.6
Ni	100 and 15 Å	1.3	14	1.2	12.7	1.7	18.5
Cu		2.3	24.9	2.0	21.8	3.3	36.1
Zi		1.3	14	1.2	12.7	1.7	18.5
Ni	150 and 10 Å	1.8	20	1.8	19.3	2.8	29.8
Cu		3.7	40.4	3.5	38.3	5.3	58.3
Zi		1.8	20	1.2	13.4	2.7	29.7

It is evident that the increase in the adsorption of the L- alanine tetramer is due to the increase in the stability of the metal complex $(L\text{-ala})_4M_2$ formed (Table 3). Further, it is observed that the number of L-species adsorbed also depends on the magnitude of the relative stabilization between the L- and the D-analogues. The DFT calculations using the polarized basis set at the B3LYP/6-31G*//B3LYP/6-31G level predict increased relative stabilities as compared to B3LYP/6-31G calculations with and without ZPE correction. The present Monte Carlo simulation reveals that the number of $(L\text{-ala})_4$ species adsorbed on a given metal electrode is highest at B3LYP/6-31G*//B3LYP/6-

31G level of calculation. Another interesting observation is that the tendency for D- species to get adsorbed is more pronounced when a racemic mixture is employed as shown in Table 6.

Adsorption of Alanine tetramer on Nickel

For a fixed number of 100 and 150 D-enantiomer molecules chosen initially, the simulation indicates that ca.1 to 3 molecules get adsorbed on the nickel surface. On the other hand, for 100 and 150 $(L\text{-ala})_4$ molecules taken inside the cube, 19 and 29 molecules are adsorbed on the Ni surface, respectively, at the B3LYP/6-31G*// B3LYP/6-31G level (Table 6). This observation reveals that adsorption of the L-alanine tetramer is more facile than the D-analogue and this behavior is attributed to additional stabilization energy for the L-alanine tetramer-Ni_2 complex, which is 48.9 kcal/mol more than that in the D-complex. The number of $(L\text{-ala})_4$ adsorbed on the nickel surface is predicted to be about 14% and 13% respectively at B3LYP/6-31G level with and without ZPE correction, as expected from the decreased relative stabilities of 38 and 33 kcal/mol.

Adsorption of Alanine Tetramer on Copper

Table 6 shows that the adsorption of alanine tetramer on copper electrode follows analogous trend as in the case of Ni electrode. However, the number of L-species adsorbed is significantly higher and ranges from 21 to 36 (when 100 alanine molecules are initially assumed) or 38 to 58 (for 150 initial molecules) whereas the corresponding number of D -alanine tetramer adsorbed is roughly 10 % of the above value. The significant increase in the adsorption of L-species is due to the large stabilization energy difference between the L- and D- alanine tetramers on copper surface. As seen from Table 3, the stabilization energy of L-alanine tetramer-Cu_2 complex is nearly twice that of the corresponding D-counterpart.

Adsorption of Alanine Tetramer on Zinc

In this case too, the number of L - alanine tetramer molecules getting adsorbed is ca. 10 times larger than the D- species as shown in Table 6. It is noticed that the number of D- and L- molecules adsorbed on zinc surface is nearly same as that on nickel surface, although the stabilization energy difference between the L- and D-alanine tetramer-Zn_2 complex is small (Table 3).

Adsorption of Racemic Mixture of Alanine Tetramer on metal electrodes

When a racemic mixture is used for the Monte Carlo simulation study, the present methodology indicates that the adsorption of D-alanine tetramer occurs rather than L-alanine on the metal surfaces (M=Ni, Cu, Zn) (cf. Table 7, as an illustrative example the behaviour of racemic mixture on Ni (conditions being 0.001V, $10A^0$ and 100 molecules). It is seen from the Supporting Information provided that the adsorption energy difference, ΔE_{ads}, follows the sequence:

$$\Delta E_{ads(Cu)} > \Delta E_{ads(Ni)} > \Delta E_{ads(Zn)}$$

ΔE_{ads} values on Copper, Nickel and Zinc are estimated as 0.002 eV, 0.004 eV and 0.00084 eV respectively. Since

$\Delta E_{ads} = E_{iconf1} - E_{iconf2}$, where E_{iconf1} and E_{iconf2} represent the adsorption energies of D- and L- species respectively, it is clear that the D-alanine (rather than L- alanine) from a racemic mixture gets adsorbed strongly on the metals in the order Copper > Nickel > Zinc. The estimated ΔE_{ads} values on Copper, Nickel and Zinc exactly match with the umbrella inversion energy of the lone pair of electrons on the amino group of the amino acids[32]. Thus it is deduced that the umbrella inversion governs the orientation and adsorption of D-alanine tetramer molecules on metal surfaces such as Cu, Ni and Zn. This

observation is rationalized on the basis of the strain experienced by the L - alanine tetramers for attaining a favorable conformation with respect to the metal surface vis a vis the competition between D- and L- species for adsorption. From the optimized structures shown in Figure 1, it may be inferred that the L-alanine tetramer is bulkier than the D-analogue, which has more stabilizing H-bonding interactions and thus possesses a compact structure. This is quantified from the molar volumes computed at the B3LYP/6-31G optimized geometries using the Gaussian software.[10] It is clear from Table 8 that (D-ala)4 is 18.6 cc/mol smaller in volume than that of (L-ala)4. Thus the approach of (D-ala)4 from the racemic mixture to the metal surface is less hindered as compared to that of the L-tetramer. A comparison of the molar volumes of the metal complexes in Table 8 also reveals that the D-enantiomer is smaller in size than the L-counterpart. It is striking to note that the difference in volumes between the L- and D- complexes follows the order Cu (28.374) > Ni (16.388) > Zn (2.832). This feature again substantiates the predicted adsorption energy differences.

Table 7 : The adsorption energy difference at an applied potential of 0.001V in the case of Nickel ; d_{total} = 10 A^0 and number of alanine molecules = 100

	ΔE_{ads} **on Nickel obtained by simulation employing the computed stabilization energies from**			
No. of steps	**B3LYP/6-31G**	**B3LYP/6-31G**	**B3LYP/6-Corrected to ZPE 31G*// B3LYP/6- 31G**	**Inference**
1	0.00033954	0.00028892	0.00046936	
2	0.00067281	0.00057309	0.00093234	Only D – Alanine is adsorbed on the metal The % of D : L on the surface is ca. 1:10
3	0.0010	0.00086164	0.0014	
4	0.0013	0.0011	0.0019	
5	0.0017	0.0014	0.0023	
6	0.0020	0.0017	0.0028	
Number of D or L species reaching the metal surface	1.3 D–Alanine 14 L–Alanine	1.2 D–Alanine 12.7 L–Alanine	1.7 D–Alanine 18.5 L–Alanine	

Table 8. Molar volume (in cc/mol) of the D- and L-enantiomers

System	Molar volume cc/mol
$(D\text{-ala})_4$	253.702
$(L\text{-ala})_4$	272.152
$(D\text{-ala})_4Ni_2$	281.468
$(L\text{-ala})_4Ni_{2\text{-}}$	297.856
$(D\text{-ala})_4Cu_2$	280.947
$(L\text{-ala})_4Cu_2$	309.321
$(D\text{-ala})_4Zn_2$	310.294
$(L\text{-ala})_4Zn_2$	313.126

The stabilization energies (Table 3) used as input parameters in the present MD simulation analysis were generated by DFT calculations in vacuum. Although solvents are expected to play important role in the stabilization energies and structures of molecules in general, our calculations for the systems under study in water medium using the Onsager model,[25-27] at the B3LYP/6-31G optimized geometries in vacuum, show only minor changes in the total energies and in the stabilization energies (Table S1 in the supporting information). The difference in stabilization energies in water as well as in vacuum for tetrameric L-alanine amounts to 1.1kcal/mol. Further, the D- and L-complexes of Zn show variations of 1.2 and 2.4 kcal/mol respectively (Table S1). In the remaining systems studied, the difference in the stabilization energies in water and vacuum is much less than 1 kcal/mol. This clearly indicates that the interactions between the solvent water and the solute molecules under study are very small. Thus it is reasonable to assume that the structure in the aqueous solution is very close to that of the corresponding vacuum optimized

structure. Thus, although the role of solvent is not included herein, the insights obtained from the present analysis are expected to be valid in solution also.

SUMMARY

The stabilisation energies of tetrameric structures of D- and L- alanine molecules at the as well as at Cu, Ni and Zn electrodes were studied using molecular dynamics simulation at B3LYP/6-31G level. These stabilization energies were employed as the input parameters in estimating the adsorption energy difference between D- and L-alanine tetrameric molecules using a novel simulation methodology. This approach, which invokes the energy ratio as the criterion, yields the adsorption energy difference between D- and L- alanine tetramic molecules on Cu, Ni and Zn. This energy difference was found to be consistent with the Umbrella inversion energy for lone pair of electrons on the nitrogen of the amino group. The new simulation technique is demonstrated to provide (i) the amount of each configuration getting adsorbed for a chosen electrode potential and (ii) the identification of the configuration in the case of a racemic mixture.

Supporting Information Available

Table S1 gives the total energies and zero-point vibrational energies in Hartree for M-M (M being Ni, Cu and Zn), D-alanine monomer, L-alanine monomer, tetramers of D-alanine and L-alanine and the metal complexes of tetramers of D and L alanine molecules. Cartesian coordinates of the optimized geometries at B3LYP/6-31G level are given in Table S2. Tables S3 to S28 contain the step-wise adsorption energy differences between D and L alanine pertaining to Ni, Cu and Zn at 0.001V, 0.01V and 0.1 V for different box lengths (10 Å and 15 Å) and two different number of molecules (100 and 150). The complete listing of the new simulation program for estimating the extent and nature of adsorbing species (in MATLAB 6.2 version) is provided.

REFERENCES

1. See for example, A.L.Lehninger, L.D.Nelson, and M.M. Cox, *Principles of Biochemistry*, 2nd edn. (1993), CBS publishers and references therein.
2. See for example, P.N. Rylander,; *Catalytic Hydrogenation over Platinum Metals*, NY, Academic Press, (1967).
3. S. Lavoie, M.A. Laliberte, P.H. McBreen, *J. Am. Chem. Soc*., **125** (2003)15756.
4. S.D. Sholl, *Langmuir*, **14** (1998)862.
5. K.R. Paserba, A.J. Gellman, *J. Chem. Phys.* **115** (2001) 6737.
6. G. Attard, *J. Phys. Chem. B.*, **105** (2001) 3158.
7. J.D. Horvath, A.J. Gellman, *J. Am. Chem. Soc*., **123** (2001) 7953.
8. X. Zhao, Hao Yan, R.G. Zhao, W.S. Yang, *Langmuir* **19** (2003)809.
9. A.D. Becke, *J. Chem. Phys.* **98** (1993)5648; C. Lee, W. Yang, R.G. Parr, *Phys. Rev. B* **37** (1988) 785. 10. M.J. Frisch, G.W. Trucks, H.B. Schlegel, G.E. Scuseria, M.A. Robb, J.R. Montgomery, Jr, T. Vreven, K.N. Kudin, J.C. Burant, J.M. Millam, S.S. Iyengar, J. Tomasi, V. Barone, B. Mennucci, M. Cossi, G. Scalmani, N. Rega, G.A. Petersson, H. Nakatsuji, M. Hada, M. Ehara, K. Toyota, R. Fukuda, J. Hasegawa, M. Ishida, T. Nakajima, Y. Honda, O. Kitao, H. Nakai, M. Klene, X. Li, J.E. Knox, H.P. Hratchian, J.B. Cross, V. Bakken, C. Adamo, J. Jaramillo, R. Gomperts, R.E. Stratmann, O. Yazyev, A.J. Austin, R. Cammi, C. Pomelli, J.W. Ochterski, P.Y. Ayala, K. Morokuma, G.A. Voth, P. Salvador, J.J. Dannenberg, V.G. Zakrzewski, S. Dapprich, A.D. Daniels, M.C. Strain, O. Farkas, D.K. Malick, A.D. Rabuck, K. Raghavachari, J.B. Foresman, J.V. Ortiz, Q. Cui, A.G. Baboul, S. Clifford, J. Cioslowski, B.B. Stefanov, G. Liu, A. Liashenko, P. Piskorz, I. Komaromi, D.J. Martin, Fox, T. Keith, M.A. Al-Laham, C.Y. Peng, A. Nanayakkara, M. Challacombe, P.M.W. Gill, B. Johnson, W. Chen, M.W. Wong, C. Gonzalez, J.A. Pople, Gaussian 03, Revision B.03, Gaussian, Inc., Wallingford CT, (2004).

11. J.B. Foresman, A. Frisch, *Exploring Chemistry with Electronic Srtucture Methods*; Gaussian, Inc.: Pittsburgh, PA, (1996).
12. C. L. Perrin, J.B. Nielson, *Annu. Rev. Phys. Chem*. **48** (1997) 511.
13. K. Müller-Dethlefs, P. Hobza, *Chem. Rev*. **100** (2000)143.
14. K.M. Specht, J. Nam, D.M. Ho, N. Berova, R.K. Kondru, D.N. Beratan, P. Wipf, R.A. Pascal, Jr., D.I. Kahne, *J Am. Chem. Soc*. **123** (2001)8961.
15. J.E. Del Bene, *Hydrogen bonding: 1. Encyclopedia of Computational Chemistry*; Schleyer, D Editor in Chief; John Wiley: Chichester, UK, **Vol.2**, (1998).
16. J.E. Del Bene, M.J.T. Jordan, *J. Mol. Struct. (THEOCHEM)* **573** (2001)11.
17. J. Ireta, J. Neugebauer, J. Scheffler, .*J. Phys. Chem. A*, **108** (2004)5692.
18. J. He, P.L. Polavarapu, *J. Chem. Theory Comput.*, **1** (2005) 506.
19. J.P. Foster, F. Weinhold, *J. Am. Chem. Soc*. **102** (1980)7211.
20. A.E. Reed, R.B. Weinstock, F. Weinhold, *J. Chem. Phys.* **83** (1985)735.
21. A.E. Reed, L.A. Curtiss, F. Weinhold, *Chem. Rev*. **88** (1988)899.
22. K.B. Wiberg, *Tetrahedron* **24** (1968)1083.
23. A.P. Scott, L. Radom, *J. Phys. Chem*. **100** (1996) 16502.
24. The experimental time of one second is realistic in a potential sweep experiment wherein $t = (E - E_i)/\nu$ where E and E_i refer respectively to the applied potential range and the initial potential. The scan rate is denoted by ν. For values of $(E - E_i)$ ranging from 0.001V to 0.1V with a scan rate of 1mV per sec to 1000mV per sec, the experimental time may range from 1 second to 1000 seconds.
25. L. Onsager, *J. Am. Chem. Soc*.**58** (1936)1486.
26. M.W.Wong, M.J. Frisch, K.B. Wiberg, *J. Am. Chem. Soc*. **113** (1991) 4776.
27. M.W. Wong, K.B. Wiberg, M.J. Frisch, *J. Chem. Phys*. **95** (1991) 8991.